

NOVEL PHASE-SHIFTING CHARACTERISTIC OF CRLH TL AND ITS APPLICATION IN THE DESIGN OF DUAL-BAND DUAL-MODE DUAL-POLARIZATION ANTENNA

W.-Q. Cao^{1, 2, *}, B.-N. Zhang¹, A. J. Liu¹, T.-B. Yu¹,
D.-S. Guo¹, and Y. Wei¹

¹Institute of Communications Engineering, PLA University of Science and Technology, Nanjing, Jiangsu 210007, China

²State Key Laboratory of Millimeter Waves, Southeast University, Nanjing, China

Abstract—The phase-shifting characteristic of a novel composite right/left handed transmission line (CRLH TL) for two frequency points is analyzed in this paper. Samples of $(90^\circ, 0^\circ)$ and $(180^\circ, 0^\circ)$ phase-shifting TLs for two frequency points (f_1, f_2) are designed and the total length of the CRLH TLs has decreased by more than 77% compared to the conventional microstrip lines. Then a four way power divider made by three Wilkinson power dividers and interconnected with the $(90^\circ, 0^\circ)$ and $(180^\circ, 0^\circ)$ phase-shifting TLs is designed to feed an antenna with two different operating modes at two different frequency bands. Four radiating patches arranging symmetrically in a loop are printed in an upper substrate and connected with the four outputs of the feed network by four copper pins. When the four rectangular patches are excited by four sources with equal amplitude and phase at f_1 , metamaterial antenna with conical beam and linear polarization (LP) is achieved; while four sources with equal amplitude but 90° phase difference for each adjacent output at f_2 leads to wideband antenna with broadside beam and circular polarization (CP). One antenna prototype with dual-band dual-mode dual-polarization property is fabricated and good agreements between simulation and measurement results are obtained. This single-feed patch antenna is valuable in wireless communications for its radiation pattern selectivity and polarization diversity.

Received 10 August 2012, Accepted 6 September 2012, Scheduled 17 September 2012

* Corresponding author: Wen-Quan Cao (cao.wenquan@163.com).

1. INTRODUCTION

Nowadays antennas with advantages of compactness, multi-band and multifunction have been widely required in various communication systems. Among them, metamaterials, including composite right/left-handed transmission line (CRLH TL) structure, negative refractive index-transmission line (NRI-TL) structure, or other periodic structures have been investigated and introduced to design novel microwave components and antennas for their unusual electromagnetic properties recently [1–10]. In [11], a single-feed dual-band dual-mode microstrip antenna is proposed based on metamaterial structure. CRLH TL theory is introduced to analyze this antenna. Based on this metamaterial structure, microstrip antennas with multi-band dual-mode and dual-polarization property are designed and realized accordingly [12, 13]. However, the bandwidths of these antenna are limited to about 1% ~ 2%.

Then a novel reconfigurable microstrip antenna with radiation pattern selectivity and polarization diversity is reported in [14]. A four way power divider made by three Wilkinson power dividers and interconnected with switches is designed to feed this antenna. By controlling the states of the switches, the antenna characteristics can be changed into two modes: metamaterial antenna with conical beam and linear polarization (LP) and wideband antenna with broadside beam and circular polarization (CP). However, fabrication with 12 switches makes such reconfigurable antenna complex in structure and expensive in cost.

Phase-shifting transmission line (TL) is widely used in the design of microwave components such as phase shifters, couplers, baluns, series-fed lines or power dividers. Conventional TLs owns a linear phase response characteristic which leads to considerably large sizes and limited functions. Then Itoh et al. proposed a concept of CRLHTLs in [15], which has led to many novel microwave components and antennas for its nonlinear phase response characteristics [16–22]. However, the balance between left-handed and right-handed frequency-bands is highly sensitive to the detailed geometrical dimensions of the CRLH TLs which makes it difficult to design arbitrary phase response by adjusting the length of CRLH TLs. This occasion wasn't changed until Lin et al. proposed a novel compact CRLH structure in [23, 24]. Such composite CRLH TLs can also minimize the side coupling which suffers little coupling effects when integrated with other components and antennas.

In this paper, the phase-shifting characteristic of the CRLH TL proposed in [23, 24] is analyzed for two frequency point case. Samples

of $(90^\circ, 0^\circ)$ and $(180^\circ, 0^\circ)$ phase-shifting TLs for two frequency points (f_1, f_2) are designed and verified accordingly in Section 2. By using the proposed CRLH TLs, a four way power divider is designed to feed an antenna with two different operating modes at two different frequency bands in Section 3. The radiating part of the antenna consisted by four radiating patches arranging symmetrically in a loop is analyzed for the two operating modes in Section 4. Then one dual-band dual-mode dual-polarization antenna prototype is fabricated. HFSS software has been used to design and optimize the proposed antenna and good agreements between simulation and measurement results are obtained. Section 5 presents the measured results and discussion. Finally, we make conclusion in Section 6.

2. PHASE-SHIFTING CHARACTERISTIC OF THE CRLH TL

The proposed CRLH TL is shown in Fig. 1, which nearly owns the same structure as given in [23, 24]. The CRLH TL unit cell consists of series interdigital capacitor and two coupling stub inductors connected to the sides of the two linear arrays of metallic vias which can be

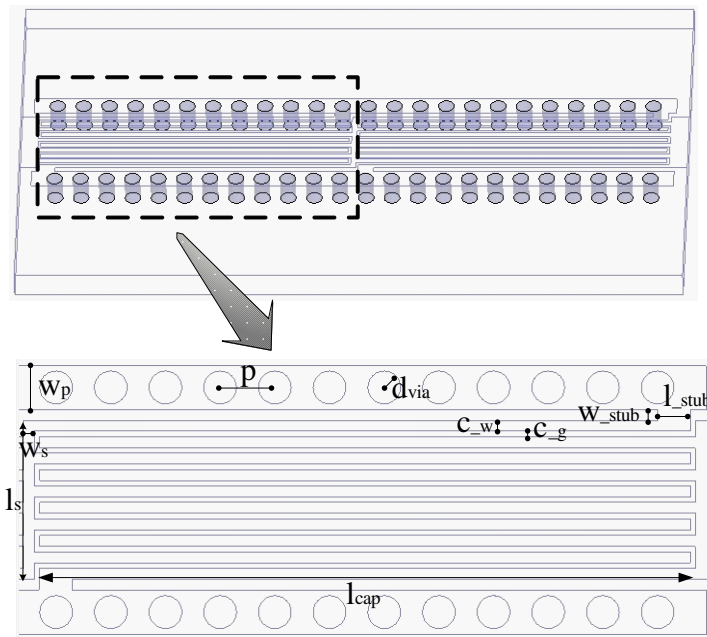


Figure 1. The structure of the composite phase-shifting TL.

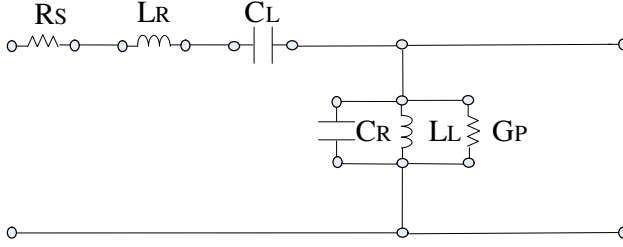


Figure 2. Equivalent circuit model for the unit cell.

regarded as electric walls. The CRLH TL is fabricated on a substrate with a thickness of h_1 and a relative permittivity of ϵ_r , $\tan \delta_1 = 0.018$. The parameters l_{cap} , l_{stub} , w_{stub} , and W_p indicate the length of the interdigital capacitor, the length and the width of the shorted stub, and the width of the side copper which is used to connect the via-walls, respectively. The sizes of the via-walls can be chosen under the following condition:

$$p/\lambda < 1/10, \quad d_{via}/p < 1/2$$

where λ is the free-space wavelength at the operating frequency, d_{via} is the diameter of vias and p is the distance between two vias.

The equivalent circuit model of each unit cell is given in Fig. 2. The left-handed components include the series interdigital capacitor C_L and the shunt stub inductor L_L which is shorted to via-walls, while the right-handed parts contain the shunt capacitor C_R and series shunt L_R which are due to the parasitic effect of the interdigital capacitor and stub inductor. R_S and G_P refer to the loss of the structure.

The novel meta-structures with via-walls own better isolation for side coupling and good balance can be achieved from the left-to right-handed band under the balance condition. Furthermore, such structure is easy to be integrated with other components. The transmission properties and phase responses for one fixed frequency point are analyzed and discussed in [23, 24].

In this paper, we firstly analyze the relation between the phase of S_{21} and the number of the unit cells n , which is shown in Fig. 3. It can be found that the phase slope was affected fundamentally by the unit cell number. Large number n leads to larger phase slope versus the frequency. For the conventional microstrip line, the phase response can be written as [25]:

$$\phi_s = -\beta l_s \approx \frac{-2\pi\sqrt{\epsilon_e}}{\lambda_0} \cdot l_s = \frac{-2\pi\sqrt{\epsilon_e} \cdot l_s}{c} \cdot f$$

where β the phase is constant of wave propagation, ϵ_e is the effective

permittivity of the microstrip line and can be expressed as [25]:

$$\epsilon_e = \frac{1 + \epsilon_r}{2} + \frac{1 - \epsilon_r}{2} \sqrt{1 + \frac{10h}{W}}$$

Thus, $\epsilon_e = 1.884$, $\phi_s(\text{deg}) = -1.647l_s \cdot f$. It can be obtained that conventional TL owns a linear phase response characteristic. Furthermore, longer line l_s leads to larger phase slope versus the frequency. So it can be concluded that, although CRLH TL owns non-linear phase response characteristic, the trends are the same for the two TLs that longer line leads to larger phase slope.

In this section we pay attention to the phase response for two different frequency points f_1, f_2 . And two samples of phase-shifting TL with $(90^\circ, 0^\circ)$ and $(180^\circ, 0^\circ)$ for (f_1, f_2) will be designed. As we can found that in Fig. 3, $f_1 = 1.48 \text{ GHz}$, $f_2 = 1.94 \text{ GHz}$ are two good valuable points for the CRLH TL case. When $n = 2$, the phase-shifting value of (f_1, f_2) for the CRLH TL is exactly $(90^\circ, 0^\circ)$; when $n = 4$, the phase-shifting value of (f_1, f_2) for the CRLH TL is exactly $(180^\circ, 0^\circ)$. In this case the optimized value of the parameters is given in Table 1 and the structures of the two are described in Fig. 4.

For comparison, the phase responses for two frequencies f_1, f_2 of

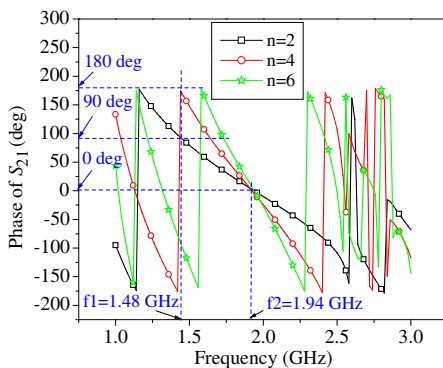


Figure 3. The phase of S_{21} versus number of the unit cells.

Table 1. Parameters values of the CRLH TL (unit: mm).

W_p	p	d_{via}	l_{stub}	w_{stub}	w_s	l_s	l_{cap}	C_g	C_w
0.8	1	0.3	0.6	0.2	0.2	2.9	13	0.1	0.2

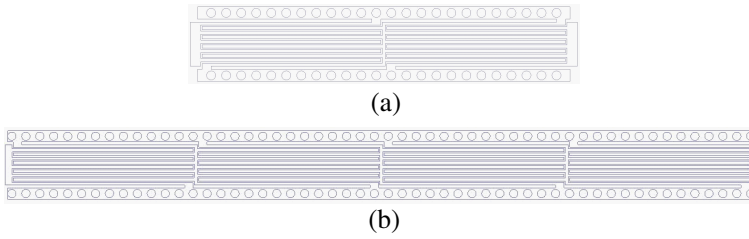


Figure 4. (a) $(90^\circ, 0^\circ)$ CRLH TL for (f_1, f_2) , (b) $(180^\circ, 0^\circ)$ CRLH TL for (f_1, f_2) .

the conventional TL can be given as:

$$\begin{aligned}\phi_s(f_1) &= -1.647l_s \cdot f_1 \\ \phi_s(f_2) &= -1.647l_s \cdot f_2\end{aligned}$$

We can get the length of the TLs from the following expression:

$$\Delta\phi_s = \phi_s(f_2) - \phi_s(f_1) = -1.647l_s \cdot (f_2 - f_1)$$

For the $(90^\circ, 0^\circ)$ case,

$$l_s = \Delta\phi_s / (-1.647 \cdot (f_2 - f_1)) = 90 / (1.647 \cdot 0.46) = 118.8 \text{ mm},$$

For the $(180^\circ, 0^\circ)$ case,

$$l_s = \Delta\phi_s / (-1.647 \cdot (f_2 - f_1)) = 180 / (1.647 \cdot 0.46) = 237.6 \text{ mm}.$$

The total length for the CRLH TLs of the two cases are:

$$\begin{aligned}l_{CRLH(n=2)} &= l_{cap} \cdot 2 + 3 \cdot W_s + 2 \cdot C_g = 26.8 \text{ mm}, \\ l_{CRLH(n=4)} &= l_{cap} \cdot 4 + 5 \cdot W_s + 4 \cdot C_g = 54.4 \text{ mm}.\end{aligned}$$

It can be found that the total length of the CRLH TLs has decreased by more than 77% compared to the conventional TL. The proposed CRLH TL owns more advantage in designing $(90^\circ, 0^\circ)$ and $(180^\circ, 0^\circ)$ phase-shifting TLs for two frequency points (f_1, f_2) in size consideration.

3. THE ANTENNA GEOMETRY AND THE FEED NETWORK DESIGN

The geometry of the proposed antenna is shown in Fig. 5. The novel antenna consists of three layers: the radiating part the network part and the air-layer in-between them. The upper layer consists four rectangular radiating patches with a length of L_p and width of W_p printed on a square substrate with a dielectric constant of ϵ_r ,

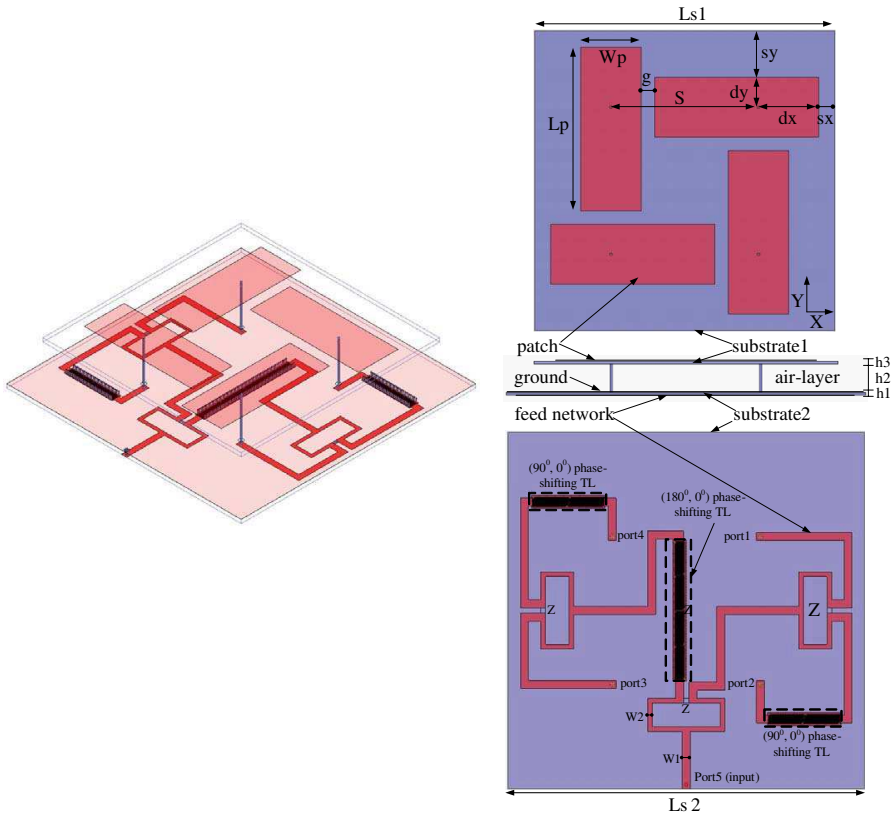
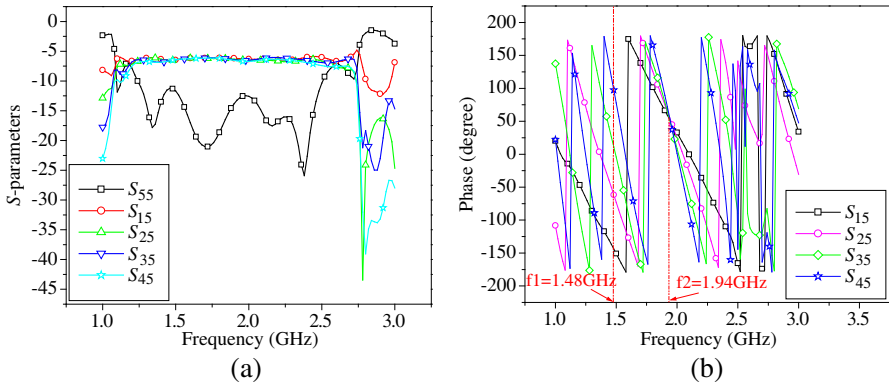


Figure 5. Geometry of the proposed antenna: 3D view; top view (radiating part), side view and bottom view (feed network) (up-down).

$\tan \delta_2 = 0.018$, height of h_3 and length of L_{s1} . The four patches are arranged in a loop structure with the center of the substrate as the coordinate center and the gap of each adjacent one is g . The down layer is a feed network made by three Wilkinson power dividers, of which the feed lines are printed on a square substrate with a dielectric constant of ϵ_r , $\tan \delta_1 = 0.018$, height of h_1 and length of L_{s2} . The four outputs of the feed network are symmetrically connected to the patch by four pins. The square ground plane with size of L_{s2} is printed on the up surface of the down-layer and an air-layer exists in between the two substrates. Four copper holes of size larger than the pin radius are etched on the ground plane to isolate the four pins. The $(90^\circ, 0^\circ)$ and $(180^\circ, 0^\circ)$ phase-shifting TLs for two frequency points (f_1, f_2) designed in Section 2 are interconnected in the feed line to control the phase of the four output sources of the feed network. Location of the pins with a distance (dx, dy) away from the edge of the radiating patch

Table 2. Parameter values of the proposed antenna (unit: mm).

L_{s1}	L_{s2}	L_p	W_p	S	sx	sy	dx	dy
110	130	60	22	54	6	17	22	11
h_1	h_2	h_3	W_1	W_2	g	Z	ϵ_r	
1	7.8	1	2.9	1.7	5	100 ohm	2.2	

**Figure 6.** S -parameters of the feeding network structure: (a) amplitude; (b) phase.

is optimized to obtain good impedance match. The optimized values for the parameters are given in Tables 1 and 2.

The proposed feed network is described in Fig. 5. Three Wilkinson power dividers connected by conventional TLs and CRLH TLs are designed to realize a four way power divider. The structure of the feed network owns nearly the same topology as that given in [14] except that $(90^\circ, 0^\circ)$ and $(180^\circ, 0^\circ)$ phase-shifting CRLH TLs are introduced to control the output phases of the four output ports. Fig. 6(a) shows that output signals of the four ports have nearly the same amplitude along the frequency band from 1.25 GHz to 2.5 GHz; Fig. 6(b) describes that the same phase is achieved for the four output ports at $f_2 = 1.94$ GHz and 90° phase difference for each adjacent port can be obtained at about $f_1 = 1.48$ GHz as is predicted. Comparing to the feed network proposed in [14], two different states of the outputs is realized without using the switches which can simple the antenna structure and decrease the fabrication cost.

4. THE RADIATING PART OF THE ANTENNA

The radiating part of the antenna is described in Fig. 5. When the input signal operates at $f_1 = 1.48$ GHz, the antenna works in broadside

mode (radiates with broadside radiation patterns).

On this occasion, four outputs of the feed network are of equal magnitude but 90° phase difference for each adjacent output and antenna works like an antenna array feeding with sequential rotation technique which can improve the bandwidth, polarization purity and the radiation pattern symmetry of antenna [26, 27]. Sequential rotation technique is a method that generating circularly polarized radiation from an array composed of linearly polarized elements having unique angular and phase arrangements. The element angular orientation and

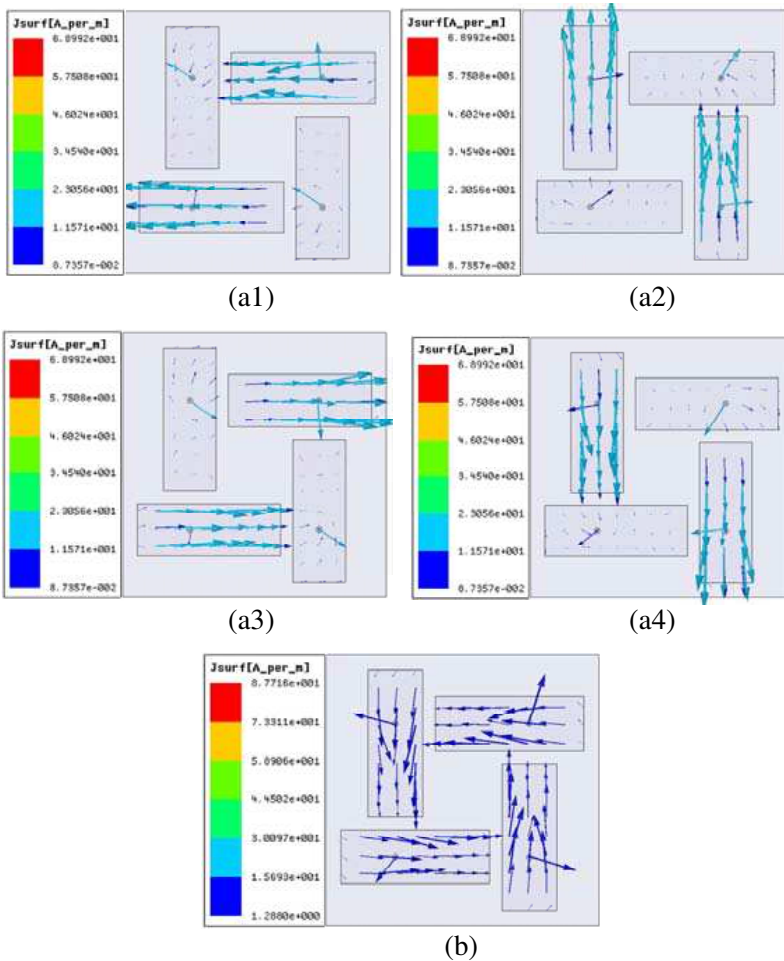


Figure 7. Surface current distributions of the proposed antenna. (a) $f_1 = 1.48$ GHz (a1) $t = 0$; (a2) $t = T/4$; (a3) $t = T/2$; (a4) $3T/4$; (b) $f_2 = 1.94$ GHz.

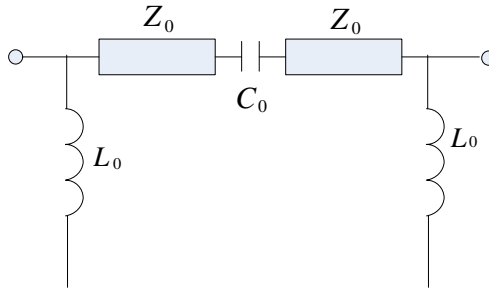


Figure 8. NRI-TL metamaterial π unit cell.

feed phase of the proposed 2×2 subarray are arranged in the 0° , 90° , 180° , 270° fashion. With such a system, not only is the feed complexity reduced, but also the bandwidth performance is improved. To verify the analysis, the surface current distributions of the CP antenna at $t = 0, T/4, T/2, 3T/4$ are described in Fig. 7(a). It can be found that the four radiating patches are operating at a CP mode exactly.

When the input signal operates at $f_2 = 1.94$ GHz, the antenna works in conical mode (radiates with conical radiation patterns). Four outputs of the feed network are of the same magnitude and phase, thus the currents in each of the radiating patch are equal in magnitude and phase which is shown in Fig. 7(b). In this occasion, the antenna is similar to a short monopole antenna, so a conical pattern with a vertical field polarization can be obtained. Actually, this antenna can be deduced from the metamaterial concept which can be found in [28, 29]. It can be considered as four metamaterial (MM) unit cells arranged in a loop structure. Each NRI-TL unit cell is shown in Fig. 8. The phase shift per unit cell, ϕ_{MTM} , can be written as: $\phi_{MTM} = \phi_{TL} + \phi_{BW} = -\omega\sqrt{LC}d + 1/(\omega\sqrt{L_0C_0})$. The total phase incurred by the host TL, ϕ_{TL} and the phase incurred by the backward-wave line formed by the series capacitive and shunt inductive loading, ϕ_{BW} . When $Z_0 = \sqrt{L_0C_0} = \sqrt{L/C}$ each MM unit cell is excited to incur an insertion phase of 0° , and series and shunt branch of the antenna resonates at the infinite wavelength mode of the same frequency with no stop band.

5. RESULTS AND DISCUSSIONS

To confirm the property of the dual-band dual-mode dual-polarization antenna, a prototype was fabricated and measured which is shown in Fig. 9. The parameters are optimized and listed in Tables 1 and 2.

Figure 10 shows the simulated and reflection coefficients of the

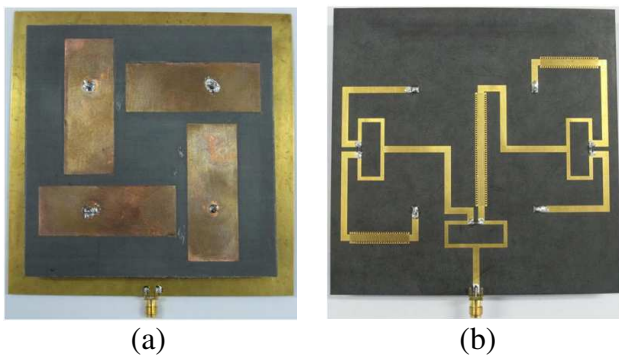


Figure 9. The photograph of the proposed antenna. (a) Top view (radiating part); (b) bottom view (feed network).

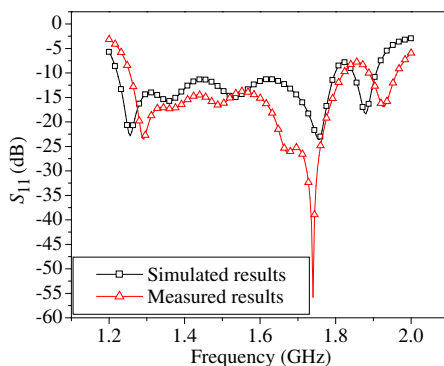


Figure 10. Simulated and measured S_{11} of the antenna.

proposed antenna. As the working principles for the two modes are quite different which are analyzed in section 4, the impedance matching of the two modes differs significantly from each other. For the broadside mode, measured results shows good impedance matching from 1.255 GHz to 1.821 GHz with -10 dB bandwidth of 36.8%, while the simulated one resonates at 1.51 GHz with -10 dB bandwidth of 38.1%. For the conical mode, measured results shows good impedance matching from 1.888 GHz to 1.962 GHz with -10 dB bandwidth of 3.8%, while the simulated one resonates at 1.88 GHz with -10 dB bandwidth of 3.3%. The measured results of both the two modes resonant at a little higher band than the simulated ones. Frequency shift may due to the tolerance exist in the antenna prototype fabrication such as the air gap with nonuniformity in-between the two substrates and the soldering effect of the copper pins.

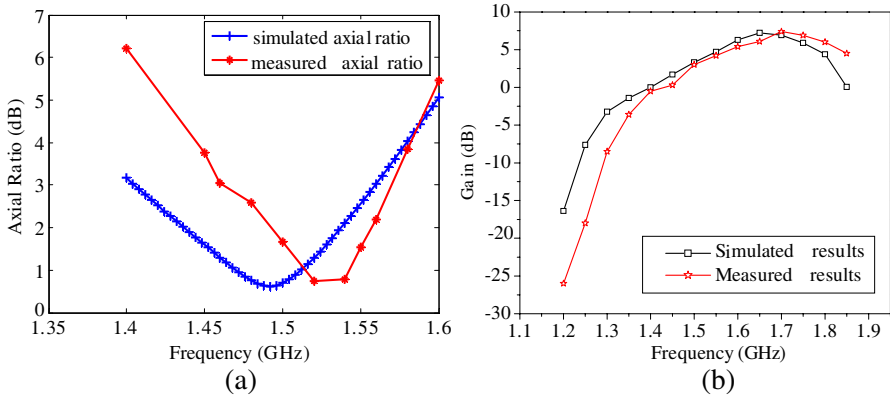


Figure 11. Simulated and measured (a) AR and (b) gain for the broadside mode.

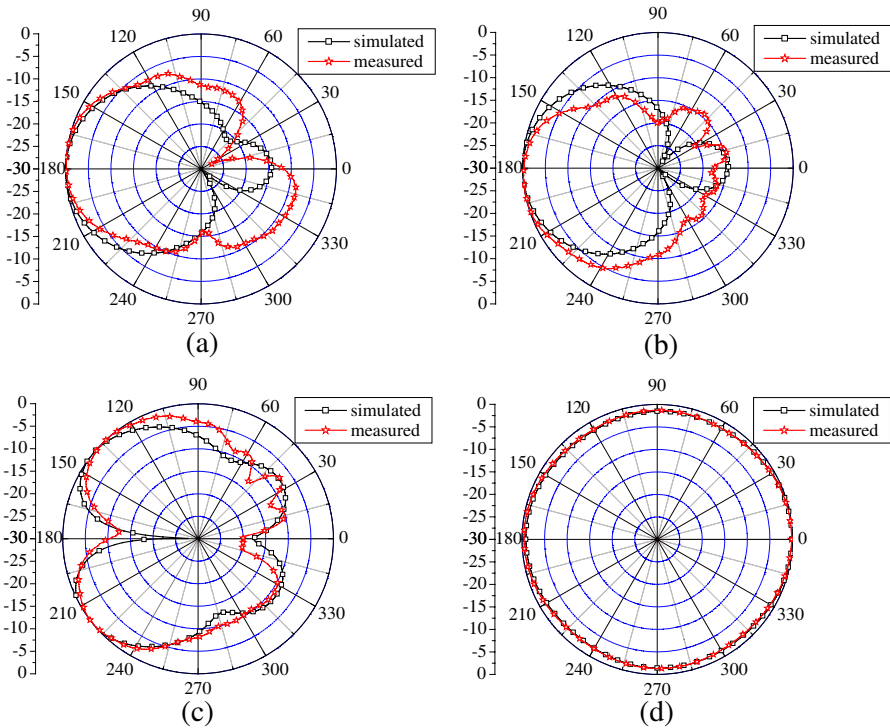


Figure 12. Radiation patterns of the proposed antenna. (a) E plane $\phi = 0^\circ$ at 1.515 GHz; (b) H plane $\phi = 90^\circ$ at 1.515 GHz; (c) E plane $\phi = 0^\circ$ at 1.928 GHz; (d) H plane $\theta = 35^\circ$ at 1.928 GHz.

As shown in Fig. 11, both simulated and measured axial ratio (AR) and gain for the broadside mode are described. Good CP property with measured 3 dB axial ratio (AR) bandwidth of 7.3% is obtained for this mode. The AR bandwidth is much narrower than the impedance bandwidth. This may be due to that the 90° phase difference for each adjacent output port is not wide enough which can be found in Fig. 6(b). Maximum gains of the antenna are 4.9 dBi and 6.9 dBi for conical mode and broadside mode respectively. Measured gain shifts a little to higher band may also due to the fabrication tolerances and the SMA effects.

Both simulated and measured radiation patterns of the E plane and H plane of the two modes are presented in Fig. 12. As shown in Figs. 12(a) and (b), patch-like radiation patterns for the broadside mode are obtained as predicted. A monopole-like radiation pattern (Omni-directional in azimuthal plane) with a null in broadside of the patch is achieved for the conical mode. The peak gain is obtained not right in the azimuthal plane but with an obliquitous angle of about 35° . Little discrepancy which exists between the simulated and measured results may attribute to the fabrication tolerances and measurement errors. The results confirm the feasibility of the proposed method in designing microstrip antenna with dual-band dual-mode dual-polarization property.

6. CONCLUSION

We analyze the phase-shifting characteristic of a novel CRLH TL for two frequency points in this paper. Samples of $(90^\circ, 0^\circ)$ and $(180^\circ, 0^\circ)$ phase-shifting TLs for two frequency points (f_1, f_2) are designed and the total length of the CRLH TLs has decreased by more than 77% compared to the conventional TLs. Then a feed network made by three Wilkinson power dividers and interconnected with the $(90^\circ, 0^\circ)$ and $(180^\circ, 0^\circ)$ phase-shifting CRLH TLs is designed to work at two different operating states at two different frequency bands. In order to confirm the property of the proposed novel four way power divider network, a dual-band microstrip antenna with LP conical radiation patterns and CP broadside radiation patterns is presented accordingly. For the broadside mode, measured results shows good impedance matching is achieved from 1.255 GHz to 1.821 GHz with -10 dB bandwidth of 36.8%. Good CP property with measured 3 dB axial ratio (AR) bandwidth of 7.3% is obtained for this mode. For the conical mode, measured results shows the antenna resonates at 1.928 GHz with -10 dB bandwidth of 3.8%. Both the simulated and measured results prove that the proposed structure and the design

procedure is an effective method to design antennas with dual-band dual-mode dual-polarization property. This antenna has potential uses in terrestrial land-mobile or other wireless applications for its novel features.

REFERENCES

1. Sievenpiper, D., L. Zhang, R. F. J. Broas, N. G. Alexopolous, and E. Yablonovitch, "High-impedance electromagnetic surfaces with a forbidden frequency," *IEEE Trans. on Microw. Theory and Tech.*, Vol. 47, No. 11, 2059–2074, Nov. 1999.
2. Yang, F.-R., K.-P. Ma, Y. Qian, and T. Itoh, "A uniplanar compact photonic-bandgap (UC-PBG) structure and its applications for microwave circuit," *IEEE Trans. on Microw. Theory and Tech.*, Vol. 47, No. 8, 1509–1514, Aug. 1999.
3. Lai, A., K. M. K. H. Leong, and T. Itoh, "Infinite wavelength resonant antennas with monopolar radiation pattern based on periodic structures," *IEEE Trans. on Antennas and Propag.*, Vol. 55, No. 3, 868–876, Mar. 2007.
4. Francisco, J. H. M., G. P. Vicente, E. G. M. Luis, and S. V. Daniel, "Multifrequency and dual-mode patch antennas partially filled with left-handed structures," *IEEE Trans. on Antennas and Propag.*, Vol. 56, No. 8, 2527–2539, Aug. 2008.
5. Niu, J.-X., "Dual-band dual-mode patch antenna based on resonant-type metamaterial transmission line," *Electronics Letters*, Vol. 46, No. 4, 266–268, 2010.
6. Dong, Y. D. and T. Itoh, "Miniaturized substrate integrated waveguide slot antennas based on negative order resonance," *IEEE Trans. on Antennas and Propag.*, Vol. 58, No. 12, 3856–3864, Nov. 2010.
7. Zhou, B., H. Li, X. Y. Zou, and T.-J. Cui, "Broadband and high-gain planar Vivaldi antennas based on inhomogeneous anisotropic zero-index metamaterial," *Progress In Electromagnetics Research*, Vol. 120, 235–247, 2011.
8. Huang, J.-Q. and Q.-X. Chu, "Compact UWB band-pass filter utilizing modified composite right/left-handed structure with cross coupling," *Progress In Electromagnetics Research*, Vol. 107, 179–186, 2010.
9. Kim, D.-O., N.-I. Jo, H.-A. Jang, and C.-Y. Kim, "Design of the ultrawideband antenna with a quadruple-band rejection characteristics using a combination of the complementary split

- ring resonators,” *Progress In Electromagnetics Research*, Vol. 112, 93–107, 2011.
10. Montero-de-Paz, J., E. Ugarte-Munoz, and F. J. Herraiz-Martinez, “Multifrequency self-diplexed single patch antennas loaded with split ring resonators,” *Progress In Electromagnetics Research*, Vol. 113, 47–66, 2011.
 11. Cao, W.-Q., B.-N. Zhang, T.-B. Yu, A. J. Liu, S.-J. Zhao, D.-S. Guo, and Z.-D. Song, “Single-feed dual-band dual-mode and dual-polarized microstrip antenna based on metamaterial structure,” *Journal of Electromagnetic Waves and Applications*, Vol. 25, No. 13, 1909–1919, 2011.
 12. Cao, W.-Q., B.-N. Zhang, A. J. Liu, D.-S. Guo, T.-B. Yu, and Y. Wei, “A dual-band microstrip antenna with omnidirectional circularly polarized and unidirectional linearly polarized characteristics based on metamaterial structure,” *Journal of Electromagnetic Waves and Applications*, Vol. 26, Nos. 2–3, 274–283, 2012.
 13. Cao, W.-Q., A. J. Liu, B.-N. Zhang, T.-B. Yu, D.-S. Guo, Y. Wei, and Z.-P. Qian, “Multi-band multi-mode microstrip circular patch antenna loaded with metamaterial structures,” *Journal of Electromagnetic Waves and Applications*, Vol. 26, No. 7, 923–931, 2012.
 14. Cao, W.-Q., B.-N. Zhang, A. J. Liu, T.-B. Yu, D.-S. Guo, and K.-G. Pan, “A reconfigurable microstrip antenna with radiation pattern selectivity and polarization diversity,” *IEEE Antennas Wireless Propag. Lett.*, Vol. 11, 453–456, 2012.
 15. Lai, A., C. Caloz, and T. Itoh, “Composite right/left-handed transmission line metamaterials,” *IEEE Micro.*, 34–50, Sep. 2004.
 16. Kim, H., A. B. Kozyrev, A. Karbassi, and D. W. van derWeide, “Linear tunable phase shifter using a left-handed transmission line,” *IEEE Microw. Wireless Compon. Lett.*, Vol. 15, No. 5, 366–368, May 2005.
 17. Mao, S.-G., M.-S. Wu, Y.-Z. Chueh, and C. H. Chen, “Modeling of symmetric composite right/left-handed coplanar waveguides with applications to compact bandpass filters,” *IEEE Trans. on Microw. Theory and Tech.*, Vol. 53, No. 11, 3460–3466, Nov. 2005.
 18. Zhu, Q., Z. X. Zhang, and S. J. Xu, “Millimeter wave microstrip array design with CRLH-TL as feeding line,” *IEEE AP-S Int. Symp.*, Vol. 3, 3413–3416, Jun. 2004.
 19. Lee, C., K. M. Leong, and T. Itoh, “Composite right/left-handed transmission line based compact resonant antennas for RF module integration,” *IEEE Trans. on Antennas and Propag.*, Vol. 54,

- No. 8, 2283–2291, Aug. 2006.
20. Mao, S.-G. and Y.-Z. Chueh, “Broadband composite right/left-handed coplanar waveguide power splitters with arbitrary phase responses and balun and antenna applications,” *IEEE Trans. on Antennas and Propag.*, Vol. 54, No. 1, 234–250, Jan. 2006.
 21. Lin, X. Q., R. P. Liu, X. M. Yang, J. X. Chen, X. X. Ying, Q. Cheng, and T. J. Cui, “Arbitrarily dual-band components using simplified structures of conventional CRLH-TLs,” *IEEE Trans. on Microw. Theory and Tech.*, Vol. 54, No. 7, 2902–2909, Jul. 2006.
 22. Gil, M., J. Bonache, J. García-García, J. Martel, and F. Martín, “Composite right/left handed (CRLH) metamaterial transmission lines based on complementary split rings resonators (CSRRs) and their applications to very wide band and compact filter design,” *IEEE Trans. on Microw. Theory and Tech.*, Vol. 55, 1296–1304, Jun. 2007.
 23. Lin, X. Q., H. F. Ma, D. Bao, and T. J. Cui, “Design and analysis of super-wide bandpass filters using a novel compact meta-structure,” *IEEE Trans. on Microw. Theory and Tech.*, Vol. 55, No. 4, 747–753, Apr. 2007.
 24. Lin, X. Q., D. Bao, H. F. Ma, and T. J. Cui, “Novel composite phase-shifting transmission-line and its application in the design of antenna array,” *IEEE Trans. on Antennas and Propag.*, Vol. 58, No. 2, 375–380, Jan. 2010.
 25. *Microstrip Circuits*, Tsinghua University and Post & Telecom Press, Beijing, China, 1976.
 26. Hu, Y.-J., W.-P. Ding, and W.-Q. Cao, “Broadband circularly polarized microstrip antenna array using sequentially rotated technique,” *IEEE Antennas Wireless Propag. Lett.*, Vol. 10, 1358–1361, 2011.
 27. Huang, J., “A technique for an array to generate circular polarization with linearly polarized elements,” *IEEE Trans. on Antennas and Propag.*, Vol. AP-34, No. 9, 1113–1124, Sep. 1986.
 28. Qureshi, F., M. A. Antoniades, and G. V. Eleftheriades, “A compact and low-profile metamaterial ring antenna with vertical polarization,” *IEEE Antennas Wireless Propag. Lett.*, Vol. 4, 333–336, 2005.
 29. Antoniades, M. A. and G. V. Eleftheriades, “A folded-monopole model for electrically small NRI-TL metamaterial antennas,” *IEEE Antennas Wireless Propag. Lett.*, Vol. 7, 425–428, 2008.